Report on the soil physics on samples collected in the Italian site

Deliverable D_3.2.4

Contributing partners:

PP1 – CNR IGG

LP – UNIPD DICEA

TABLE OF CONTENTS

1. Introduction

The project “Monitoring Sea-water intrusion in coastal aquifers and Testing pilot projects for its mitigation” (MoST) funded by the Italy – Croatia 2014 – 2020 CBC Programme aims at testing solutions against saltwater intrusion in agricultural areas.

Saltwater intrusion is a worldwide problem exacerbated by human activities and climate changes and MoST focuses on two study areas: the Veneto Region coastal plain located south of the Lagoon of Venice (Italy) and the Neretva river mouth (Croatia).

This report represents the deliverable D_3.2.4 “Report on the soil physics on samples collected in the Italian site”, issued for Action 3.2 “Laboratory investigations” within the WP3 “Studying”.

PP1-CNR characterized the geological, geomorphological and hydro-stratigraphic units in the Italian study area through the analysis of sediment cores and subsoil sampling. Sedimentological and stratigraphic approach including facies analyses was used to recognize and characterize the shallow aquifer system. Special attention was paid to identify the presence of buried sandy geomorphological bodies and the sedimentological constraints in the hydrostratigraphic setting influencing the groundwater dynamics. Results obtained were reference for saltwater intrusion monitoring, planning mitigation measures, and the implementation of the numerical modeling.

The LP carried out soil hydraulic, physical, and chemical analyses (M/S) on samples collected in the field monitoring sites. The chemical composition of groundwater samples has been also characterized on a number of samples collected in the field.

1. Materials and methods

1.1 Sediment core and field sampling

The subsoil characterization was carried out by the analysis of i) sediment cores available from previous projects, ii) new sediment cores, iii) subsoil samples taken during the excavation work for the positioning of the drainage pipe.

1.1.1 Sediment cores available from previous projects

With the aim of providing a preliminary stratigraphic reconstruction of the subsurface and planning new investigations for the MoST project, five 20-m-long cores taken as part of a previous project (GeoRisk) were used. These cores, available at CNR laboratories and never before analyzed, provided excellent support for the preliminary hydrostratigraphic and depositional reconstruction of the subsurface in the Italian pilot area. The five sediment cores, namely S1, S2, S3, S4, S5, were drilled on a complex paleochannel system. Specifically, S2, S3, S4 and S5 were taken in two main paleochannel bodies, whereas S1 was taken just outside of the easternmost one (Fig. 1).

Fig. 1- Location of sediment cores S1, S2, S3, and S5 in the Italian pilot test site. Yellow lines highlight the presence of sandy geomorphological bodies.

Tab. 1 summarizes the core positions with respect to the geomorphological features. S4 and S5 stratigraphy are assumed very similar since their proximity.

Tab. 1 - Geomorphological features of the drilling sites.

core	Site
S1	Outside the paleochannel PC1
S2	Paleochannel PC2
S3	Paleochannel PC1
S4	Paleochannel PC1
S5	Paleochannel PC1

1.1.2 Sediment cores taken within the MoST project.

MoST sediment cores were taken based on the preliminary hydrostratigraphic model made through data from available cores. At the end of May 2020, five 20-m-long cores where taken based on the following considerations:

1 Position of the sediment cores available from past projects;

2 Position of the sandy paleochannel system;

3 Position of the sub-irrigation pipe planned for the mitigation of saltwater contamination.

4 Setting up of the groundwater monitoring network in the pilot site.

The map with the positions of the new MoST sediment cores is shown in Fig. 2. Some pictures of the core sites and core line samples are reported in Fig. 3.

Fig. 2- Location of sediment cores MoST 1-5 in the Italian pilot test site. Yellow lines highlight the presence of sandy geomorphological bodies.

Fig. 3 – Example of drilling operation and core samples.

The analysis of the sediment cores consisted in: i) describing for each layer texture, structures, macrofossil content, and ii) identifying the position of the main aquifers. In addition, selected samples were taken for laboratory analysis with the aim to better characterize the depositional environments and to define a precise chronostratigraphic constraint to the stratigraphic model.

On March 24th 2021, in order to collect more stratigraphic data on the surficial subsoil of the Test area, five more sedimentary cores were recovered using an Eijkelkamp hand auger, through a gouge sampler with a length of 1 m and a diameter of 30 mm. The cores, up to 1.5 m long, were collected at the southern margin of the Test Site: GH06 next to the terminal part of the sub-irrigation system, GH01, GH02, GH03 and GH05 in the agricultural field just south the one interested by the test (Fig. 4). All cores were taken along the main path of the surficial sand body interpreted as paleo-channel, with the exception of the GH01, which was taken just outside the surficial sand body.

Subsequently, the sediment cores were cut longitudinally, described, photographed, and-samples were taken for lab analysis.

Sedimentological analyses were carried out following the basic principles of facies analyses: recognition of different sedimentary features, sediment grain size and color, presence of sedimentary structures, bioturbation and occurrence of plant and/or shell remains.

On 22 September 2020, during the excavation of the trench for the positioning of the sub-irrigation pipe, detailed observation of the soil profile along the trench down to about 1.5-1.7 m depth and sediment sampling were carried out (Fig. 4).

Fig. 4 – a) location of the surficial sedimentary cores and position of the trench used for the installation of the sub-irrigation pipe (red line); b) and c) phots of the digger at work and the trench.

1.2 Sedimentological analysis

1.2.1 Sediment core description

After the preliminary sediment core description performed in the field, selected samples were analyzed in the CNR Sedimentological Lab (Fig. 5).

The analysis consisted in the characterization of each subsoil layer by the detailed observation of texture, structures and macrofossil content. Results of sediment core analysis are summarized in lithostratigraphic logs.

Fig. 5 – Activity at CNR lab: Core splitting, samples description and preparation for sedimentological analysis.

1.2.2 Micropaleontological analysis

With the aim of determining the depositional environment of the sediments, samples for from the sediment core Most 2 and the trench were collected in order to carry out micropaleontological analysis along with a detailed sedimentological description (Fig. 6 and Tab. 2). About 50 g of sediments for each sample were soaked into water for a few hours and then washed through a stainless steel sieve with mesh openings of 63 microns (Fig. 7).

Fig. 6 – Sediment sampling for micropaleontological analyses.

Tab. 2 - - Samples for micropalaeotological analyses.

Site	Type	Depth (m)
D9	trench	0,6
D10	trench	0,68
MoST2	core	1,5
MoST2	core	1,85
MoST4	core	1,5
S1	core	1,41
S5	core	1,27
S5	core	2,32

Fig. 7 – Preparation of a sample in the Laboratory.

The samples were rinsed with milliQ water, filtered, and put in the oven at 50°C for 12 hours. The remnants on the sieve were a concentration of sand-sized material, including fossils and vegetal remains. The residue fractions with size > 125 µm were analyzed under the stereomicroscope to classify the benthic foraminiferal species.

Benthic foraminifera are unicellular protozoa with calcareous test that live in marine and brackish environments. Their shells are preserved into the sediments and may be used to reconstruct the environmental conditions of the past. Samples for chronostratigraphic analyses from the sediment core Most 2 and from the excavation of the trench were collected to complete the paleoenvironmental reconstruction of the study area.

2. Results

2.1 Hydro-stratigraphy: Sediment core S1, S2, S3, S5

Detailed stratigraphic logs derived from lithological and sedimentological analysis of S1, S2, S3 and S5 cores are shown in Fig. 10.

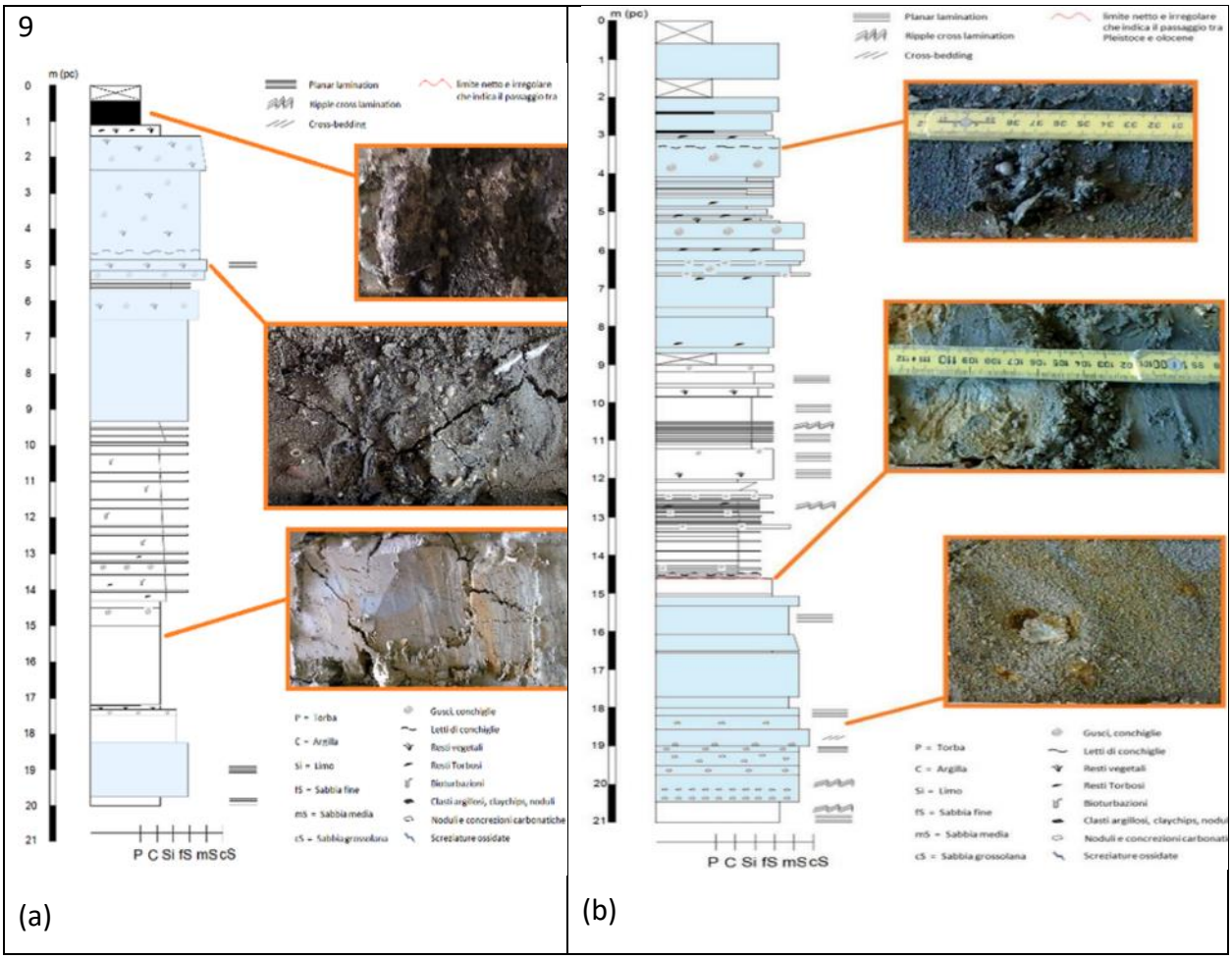

Fig. 8 – Lithostratigraphic log of and aquifers position (in light blue): a) Core S1, b) Core S2. See Fig. 1 for the drilling locations.

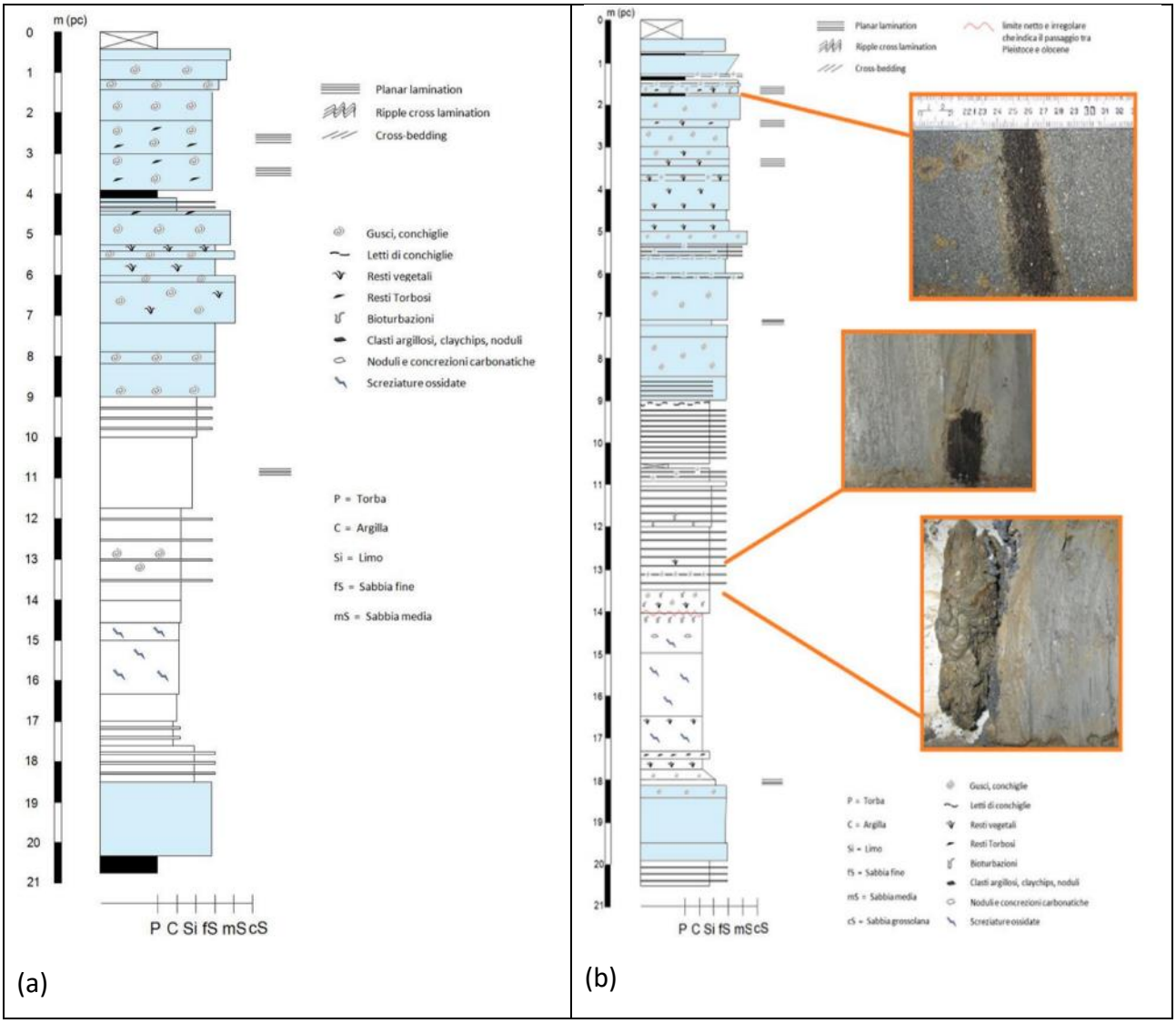

Fig. 9 – Lithostratigraphic log of and aquifers position (in light blue): a) Core S3, b) Core S5. See Fig. 1 for the drilling locations.

Lithostratigraphic analysis of sediment cores S1, S2, S3 and S5 highlighted the presence of two aquifers separated by silty and clayey layers generally, about 8-10 m thick, whose top ranges between 15 and 18 m depth (Tab. 3).

The low permeability layers gives the deeper aquifer the characteristics of local semi-confinement.

Tab. 3 – Position of the aquifers.

Sediment core	**Surficial aquifer**		**Aquitard**		**Semi-confined aquifer**
	Top depth (m)	**Bottom depth (m)**	**Thickness (m)**	**Characteristics**	**Top depth (m)**
S1	-1.4	-9.3	8.9	Silty and clayey layers	-18.2
S2	-0.6	-8.7	5.0	Silty layers and fine sand lamination in clay layers	-15.0
S3	0.0	-9.0	9.5	Clayey and silty layers	-18.5
S5	0.0	-9.0	9.4	Clayey layers with thin interbedded sandy layers	-18.4

2.2 *Hydro-stratigraphy: Sediment cores MoST1, MoST2, MoST3, MoST4, MoST5*

Five new sediment cores, namely MoST1, MoST2, MoST3, MoST4 and MoST5, specifically taken in the Italian pilot site (Fig. 2) were analyzed. The results are summarized in the stratigraphic logs reported in Fig. 10.

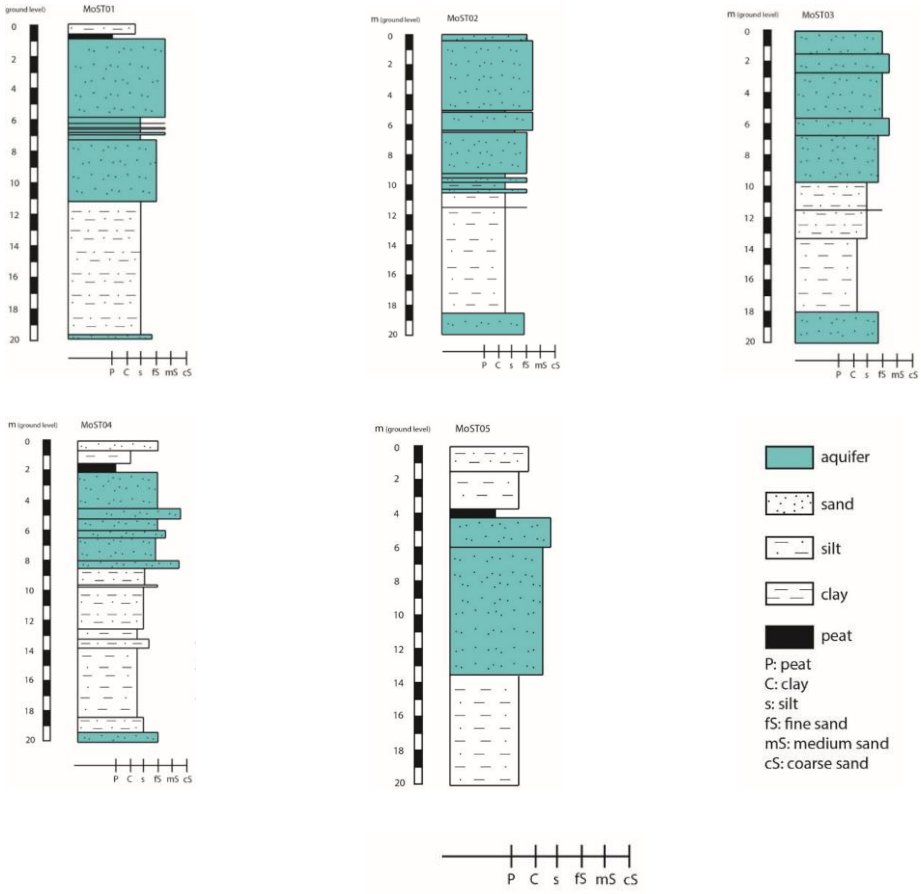

Fig. 10 – Lithostratigraphic log of core MoST1, MoST2, MoST3, MoST$, MoST5. The aquifers position is shown in light blue (see cores locations in Fig. 2).

Similar to sediment cores S1, S2, S3, S5, MoST cores also showed the presence of two main aquifer bodies separated by silty clay layers. Tab. 4 summarizes the position of the aquifer.

Tab. 4 – Position of the aquifers.

Sediment core	Surficial aquifer		Aquitard		Semi-confined aquifer
	Top depth (m)	Bottom depth (m)	Thickness (m)	Characteristics	Top depth (m)
MoST1	-0.9	-11.1	8.7	Clay and sandy silt layers	-19.8
MoST2	0.0	-10.3	8.3	Clayey layers	-18.6
MoST3	0.0	-9.7	8.3	Silts and clays layers	-18.0
MoST4	-2.1	-8.4	9.4	Silts and clay layers	-18.4
MoST5	-4.1	-13.6	9.4	Clayey layers	-

2.3 Detailed surficial sub-soil stratigraphy

Excavation of the trench made for the installation of the sub-irrigation pipe at a depth of about 1.7 m allowed detailed observation of the soil profile and collection of numerous undisturbed samples.

Four different layers were identified:

- Layer A consists of agricultural sandy-silty soil with roots, brown in colour, with a mean thickness of 0.50 m.
- Layer B consists of dark brown peat, with a thickness ranging from 0 to 0.20 m, showing a lenticular pattern.

- Layer C is made up of medium-fine yellow sand, with mottling and traces of oxidation, roots and organic remains.
- Layer D consists of medium-fine well sorted, micaceous sand, with marine mollusk shells (*Glycymeris, Turritella, Chamelea, Gibbula*), grey in color.

The stratigraphic section showing the lithological characterization of shallow subsoil, is described in the following paragraph and reported in Fig. 11.

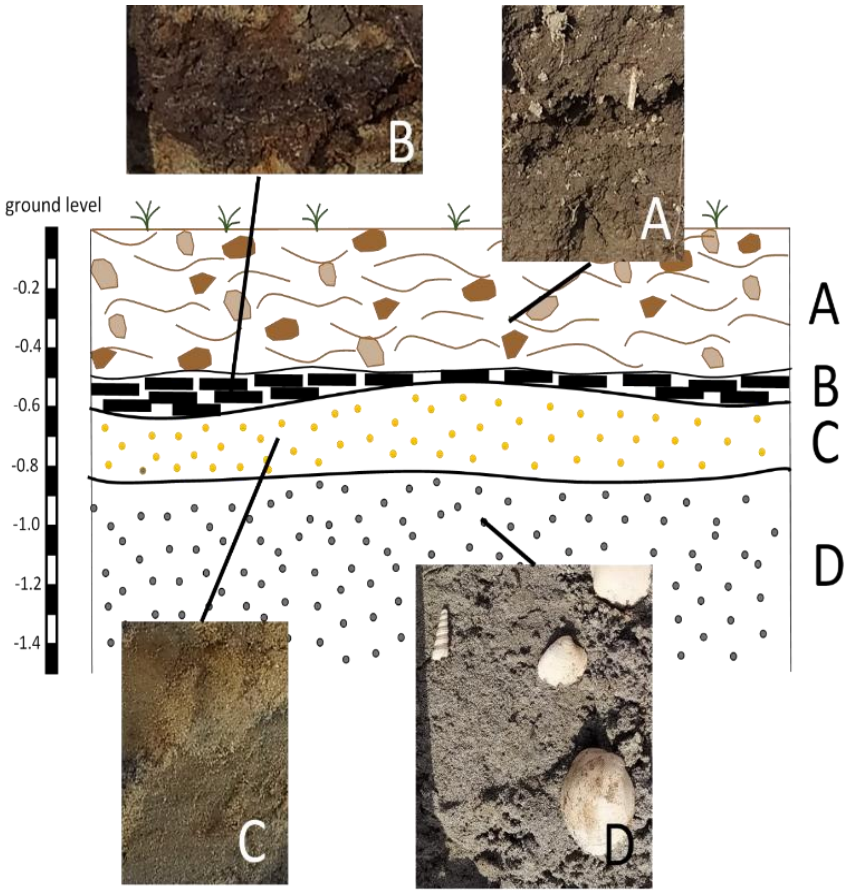

Fig. 11 – Sketch of subsoil of the first 1.5 meters.

The subsoil stratigraphy was further investigated through the analyses of six additional surficial sedimentary cores (Fig. 12):

- GH01: 0-0,10 m: brownish silt (agricultural soil); 0,1-0,5 m: silty clay passing upward to peaty clay; 0,5-1,20 m: fine to medium fine well sorted grey sand with rare vegetal remains; 1,20-1,25 m: peat layer; 1,25-1,40 m: grey sandstone with shell fragments.
- GH02: 0-0,30 m: fine sand (agricultural soil); 0,30-0,60 m: fine to medium/fine yellow sand with mottling and traces of oxidation and vegetal remains; 0,60-1 m: fine to medium/fine well sorted grey sand.
- GH03: 0-0,5 m: fine sand (agricultural soil) peaty at the base; 0,5-0,7 m: fine to medium/fine yellow sand with mottling and traces of oxidation; 0,7-1 m: fine to medium/fine well sorted grey sand.
- GH05: 0-0,4 m: peaty fine sand (agricultural soil); 0,4-0,9 m: fine to medium/fine yellow sand with mottling and traces of oxidation and vegetal remains; 0,9-1,0 5m: fine to medium/fine well sorted grey sand, with vegetal and peaty remains; 1,15-1,20 m: peat layer; 1,20-1,50 m: grey sandstone with shell fragments.
- GH05 bis (collected at the bottom of a ditch): 1-1,25 m: grey well sorted sandstone; 1,25-1,40 m: alternating peat layers and fine sand with vegetal remains.
- GH06 (collected at the bottom of a ditch): 1,25-1,45 m: grey sand with shell fragments, abundant at the base of the layer; 1,45-1,50 m: peat layer; 1,50-1,55 m: grey sand with shell fragments.

Both stratigraphic reconstructions resulting from the direct observation into the trench and from the recovery of the surficial stratigraphic cores highlighted the transition between marine to continental paleo-environment, suggested by the superposition of 4 facies (from the bottom to the top):

- Well sorted grey sand with shells and shells fragments,
- Peat or peaty clay layers (locally),
- Grey to yellow sand with vegetal remains,
- Agricultural soil.

Fig. 12 - Sedimentary cores collected in the surficial subsoil.

2.4 Micropaleontological Analyses

With the aim of better characterizing the stratigraphy in the part of the subsurface affected by the mitigation, investigations were conducted on the samples taken in the first few meters of the subsurface.

The analyses revealed a microfossils assemblage consisting of benthic foraminifera. Specifically, *Ammonia beccarii* (Linnè) is the dominant species with abundance between 60% and 76%. The content of *Buccella frigida* (Cushman) is beween 5% and 17%, *Cribrononion granosum* (d'Orbigny) 4% - 7%, *Valvulineria perlucida* (Heron-Allen & Earland) 4% - 5%, *Haynesina paucilocula* (Cushman) 1% - 7%. Few other species are present and reach a total content of 5% (Fig. 13).

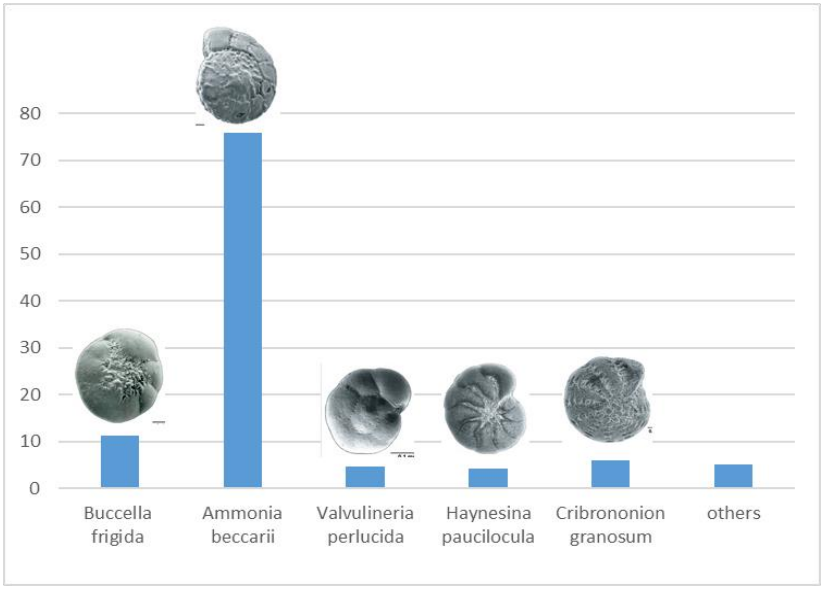

Fig. 13 - The mean composition of foraminiferal assemblages found in sandy samples at depths between 0.60 and 1,50 m.

In this foraminiferal assemblage, tolerant species of coastal and estuarine environment are present. In particular, this assemblage can be referred to the outer lagoon biotope, which currently occupies part of the southern Venice lagoon (Albani et al., 2007). In the analyzed samples the species B. frigida, together with very few planktonic foraminifera, indicates an active exchange with the sea water.

2.5 Facies analysis and spatial correlation

Based on the collected data, especially the core S1-S5 and MoST1-MoST5 log description, the upper 20 meters of the subsoil was investigated in terms of facies analysis in order to reconstruct the paleonvironmental evolution of the site (Fig. 14) and to better understand the relationship between stratigraphy and hydrogeology. Finally, two hydrostratigraphic sections, one along and one perpendicular to the sub-irrigation system were made, i.e. along the surficial sand-body (Fig. 16).

2.5.1 Facies association

In the studied succession, seven facies associations (FA1-FA) were distinguished, each one corresponding to a different step in the paleo-environmental evolution of the area (Fig. 14).

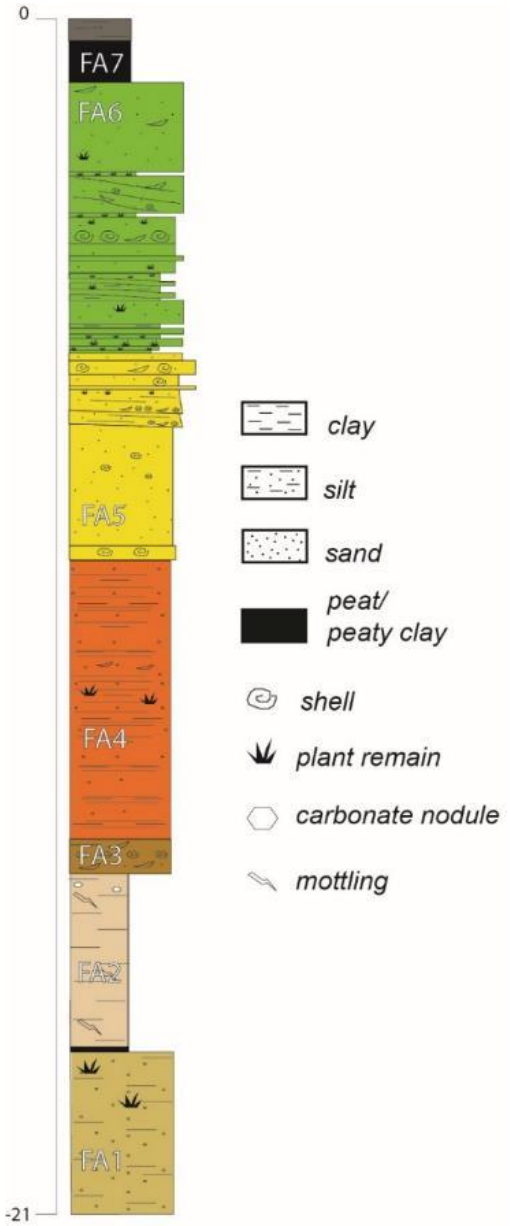

Fig. 14 – Stratigraphic column representative of the studied sedimentary succession. The section drawn summarizes the stratigraphy of the studied area and it is not linked to any particular core.

- **FA1:**

  Description: brownish-greysh sandy silt to silty sand, locally presenting vegetal remains.

  Interpretation: Pleistocene (LGM) alluvial sand and silt.

  Hydrology: Confined aquifer

- **FA2**:

  Description: light brown clay to silt, highly compacted, with mottling and carbonate nodules and other signs of pedogenesis. FA2 has a mean thickness of 3m.

  Interpretation: This layer of fine-textured alluvial deposits altered and consolidated is referred to as the Caranto paleosol (Donnici et al., 2011). The top of this unit marks the Pleistocene/Holocene boundary, and represents a stratigraphic hiatus.

  Hydrology: Aquiclude

- **FA3:**

  Description: grey silt to silty sand deposits, structurless, with abundant shells and shell fragments from lagoonal (at the base) to marine (in the upper portion). The base of this unit is marked by an erosional surface. FA3 present a mean thickness of about 0,5-1m.

  Interpretation: back-barrier to barrier deposits. The erosional surface has been interpreted as a ravinement surface, indicating the marine ingression.

  Hydrology: Aquifer

- **FA4:**

  Description: alternation of millimetric to centimetric thick layers of grey silt and sandy silt. It shows planar to cross laminations, rare vegetal remains, cm-thick sandy layers with

marine bivalves, gastropods and shell fragments. This facies association present a mean thickness of 4 m.

Interpretation: lower shoreface – prodelta deposits.

Hydrology: Aquitard

- **FA 5**:

  Description: fine to medium sand showing abundant shells and shell fragments and vegetal remains. The lower portion of the unit is characterized by a higher sorting than the upper portion. At the base of this unit, in the majority of the studied cores, a shell lag was found. The thickness varies from 4 to 9 m approximately.

  Interpretation: This unit is interpreted to be deposited in an upper shoreface (beachface) environment, testifying the progressive progradation of sediments from land to sea. The shell lag at the base of the unit is possibly related to the maximum flooding surface (corresponding to the innermost position reached by the sea).

  Hydrology: Aquifer

- **FA 6:**

  Description: Sand to silty sand with vegetal remains, particularly abundant at the base, and rare shells and shell fragments. These sediments contain a microfossils assemblage consisting of benthic foraminifera (*A. beccarii, B. frigida granulate, C. granosum, H. paucilocula*) of coastal and estuarine environment, possibly of outer lagoon. This facies association is discontinuous in the subsoil of the studied area, presenting a maximum thickness of 4 m.

Interpretation: This unit corresponds to the surficial geomorphological sandbodies, and it is interpreted to be deposited in a lagoon environment, specifically within a tidal channel.

Hydrology: Aquifer

- **FA7:**
- Description: discontinuous deposits of the uppermost subsoil layer, immediately below the arable land. Fa7 contains peat, peaty clay layers or clay levels with abundant vegetal remains. This discontinuous layer reach a maximum thickness of 4 m, where present.
- Interpretation: this facies testifies the occurrence of the marsh environment existing in the area before the hydraulic reclamation, occurred at the beginning of 20th centuary.
- Hydrology: aquiclude

Facies associations from FA3 to FA7 record the Holocene transgressive-regressive cycle, in accordance with the regional stratigraphic reconstruction reported by many authors (e.g., Bonardi et al., 2006).

The described succession is well framed in the regional subsoil models already reconstructed in the literature (Tosi et al., 2007; Tosi et al., 2009; Zecchin et al., 2008; Zecchin et al., 2009; Zecchin et al. 2011).

2.5.2 Stratigraphic Sections

On the base of the facies analyses, two perpendicular stratigraphic sections of the subsoil of the MoST site have been sketched (localized in Fig. 15 and reported in Fig. 16). FA1 to FA4 are quite homogeneous in thickness and depth, while the upper part of the subsoil, corresponding to the phreatic aquifer is characterized by etheropic relationship between different stratigraphic bodies. In particular FA2 is discontinuous, forming a net of lenticular sand bodies, resting on the

littoral sands of FA3. These two facies associations together form the phreatic aquifer. FA1 locally forms an impervious layer at the very top of the succession.

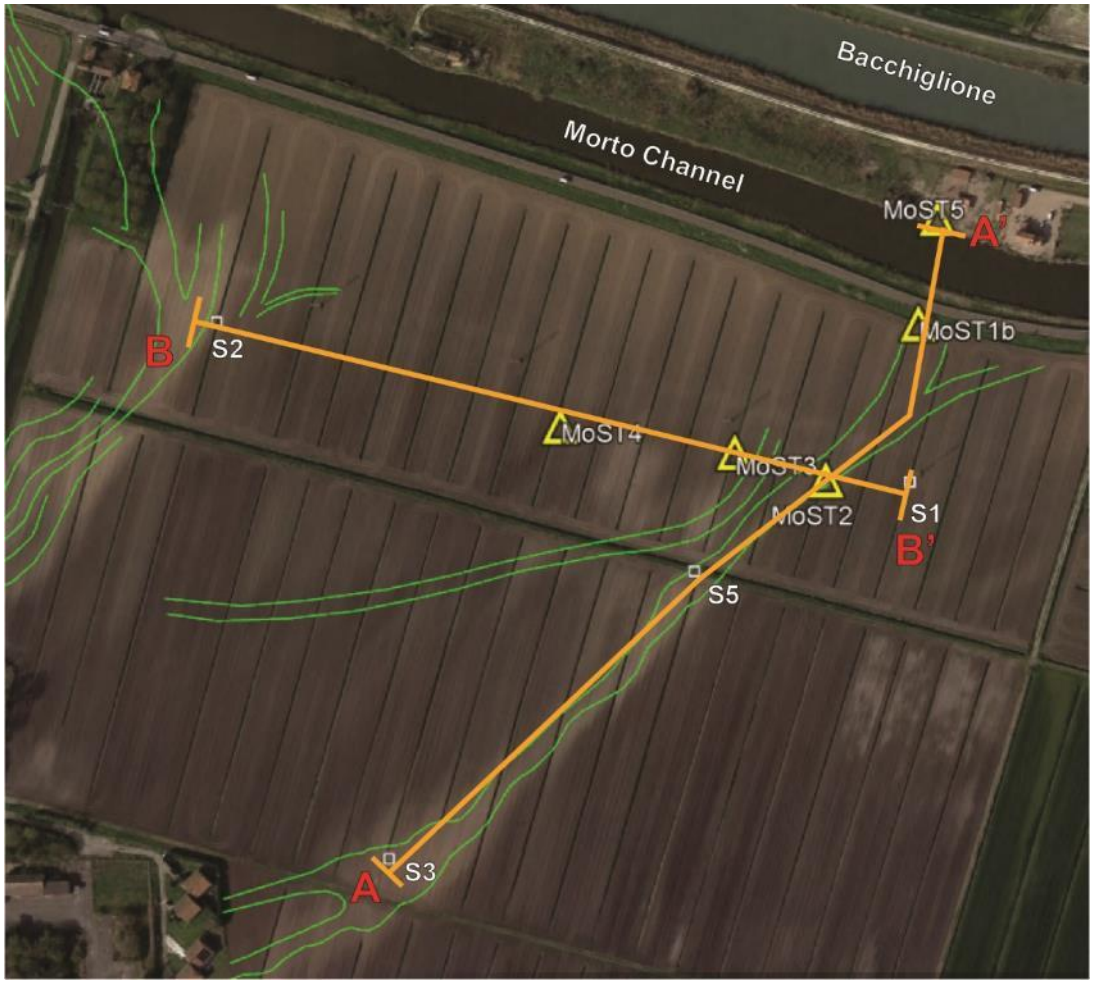

Fig. 15 – Map of the test site reporting the localization of the two stratigraphic sections (A-A', B-B'). The surficial sandy geomorphological bodies are indicated with green lines. The yellow triangles represent the MoST1-MoST5 wells, while the white squares the S1-S5 wells.

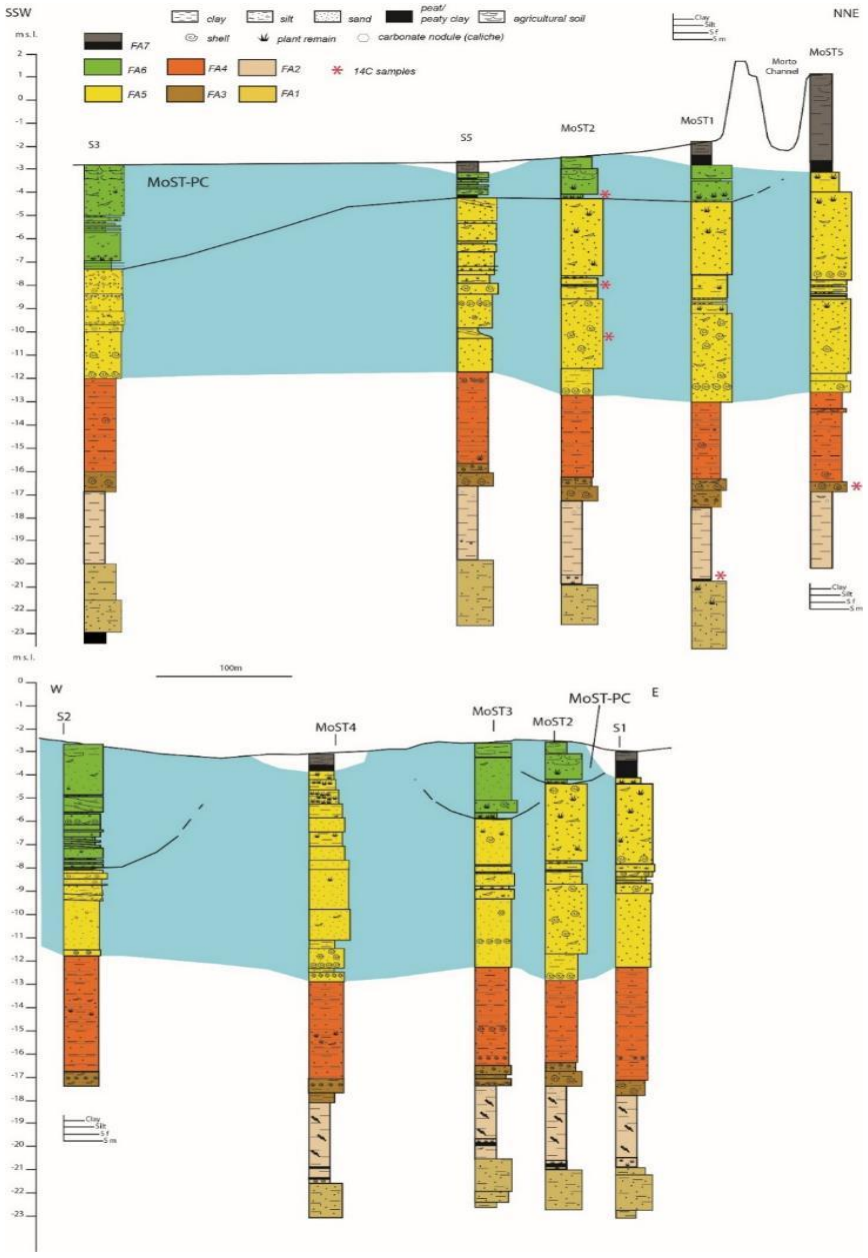

Fig. 16 – Stratigraphic sections of the pilot test site: A-A') along the surficial sandy paleo-channel (SSW-NNE direction); B-B') perpendicular to the paleochannel (W-E direction). In light blue is indicated the phreatic aquifer of the site.

3. Physical and chemical lab analyses on soil and groundwater samples

3.1 Soil hydraulic, physical, and chemical analyses (M/S)

A monitoring network was established in 2019, 2020, and 2021 to assess the groundwater dynamics inside and outside the main sandy paleochannel and quantify the effects of the freshwater recharge through the ~200-m long-buried pipe drain installed in September 2020. The network consisted of five monitoring stations (S) equipped with one 2.5 m deep piezometer for groundwater monitoring (water table, electrical conductivity, and temperature), and soil sensors installed at 0.1, 0.3, 0.5, and 0.7 m depths for soil moisture, matric potential, ECa, and temperature monitoring. Three of these stations were placed along the paleochannel (S1, S2, S3), while S4 and S5 were placed outside about 30 m away. Moreover, six additional 2.5 m deep piezometers (P) were installed at 5, 10, and 20 m from both sides of S2 in 2021 only (Figs. 30 and 31).

A sampling campaign was performed at each monitoring position (S) to assess soil hydraulic, physical, and chemical characteristics both inside and outside the main sandy paleochannel.

Fig. 30 Experimental site and position of the monitoring stations.

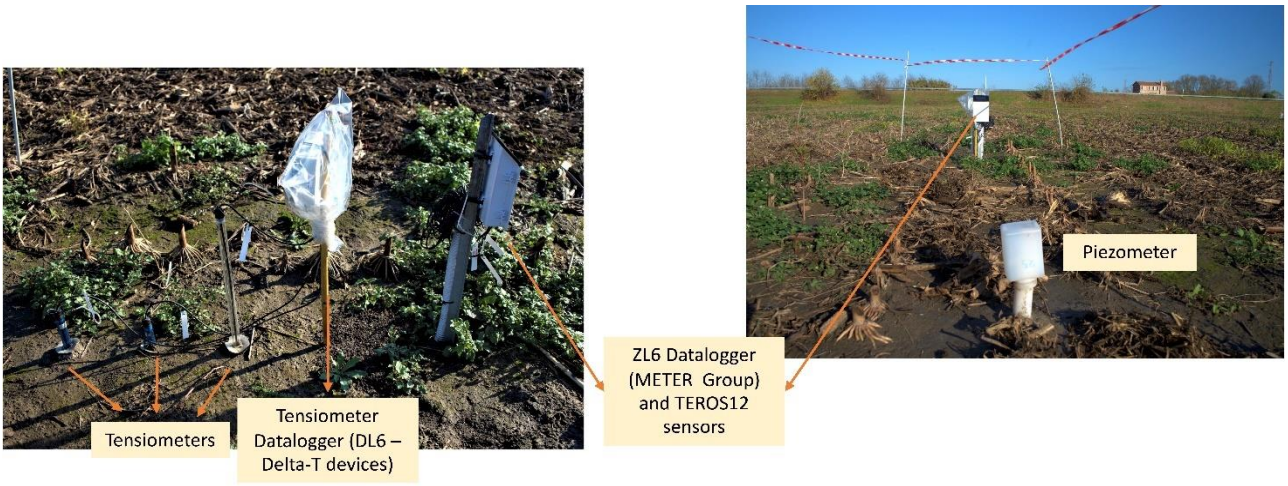

Fig. 31 Picture of the monitoring station with soil sensors, data loggers, and piezometers. The soil moisture, EC, and T sensors are not visible because they are completely into the soil.

The hydraulic characterization of the pilot site was performed by assessing the soil water retention curves (SWRCs), which describe how water is stored and its possibility to flow in the unsaturated zone above the water table, and the saturated hydraulic conductivities (K_s), which describes how easily water can pass through the soil in a saturated condition, i.e. below the water table.

With the aim of determining SWRCs and K_s, undisturbed soil samples (Fig. 32) were collected before and after the installation of the drain infrastructure (June 2020 and June 2021) using a hydraulic core sampler. At each location, two types of core samples (8 cm diameter, 5 cm height, and 5 cm diameter, 2.5 cm height) were extracted at four depths referred to their mid-point (0.1, 0.3, 0.5, and 0.7 m). Saturated hydraulic conductivity was measured using a laboratory permeameter with ascendant water flow (Eijkelkamp, Giesbeek, The Netherlands). Retention curves were determined using the sandbox (Eijkelkamp, Giesbeek, The Netherlands) from -1 to -7 kPa, the Richards' plates for -30 kPa and - 500 kPa, and the WP4 dew-point potentiometer from -100 to -2000 kPa. After the hydraulic analyses, the samples were oven-dried at 105° for 24 hours to determine the dry weight and bulk density (BD). Two examples of the SWRCs and K(h) (i.e., the relationship between hydraulic conductivity and water potential) curves derived by interpolating the lab data with the van Genuchten-Mualem model (Mualem, 1976; van Genuchten, 1980) are given in Fig. 33.

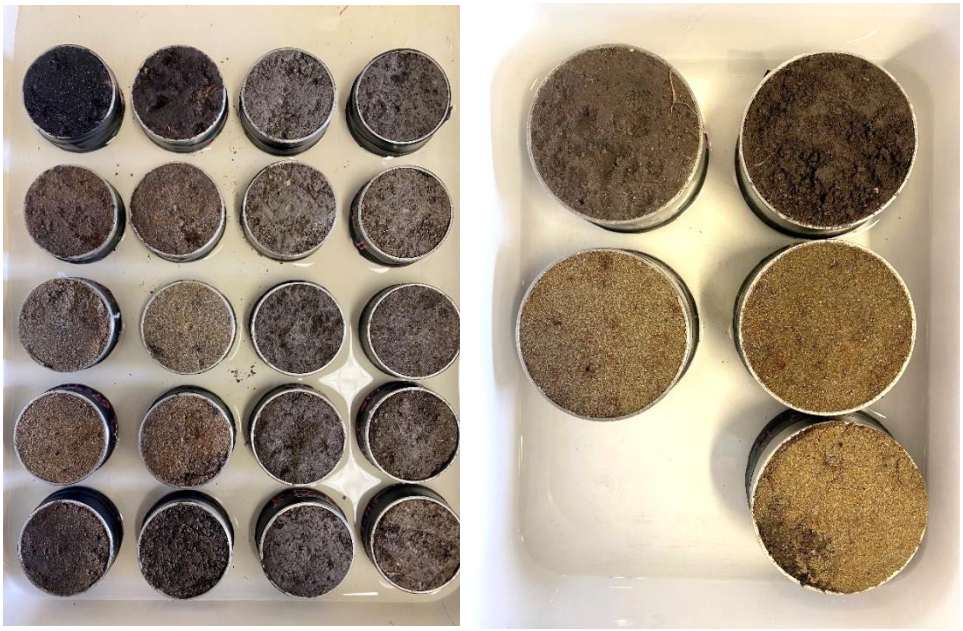

Fig. 32 Undisturbed soil cores collected at the pilot site with the hydraulic core sampler.

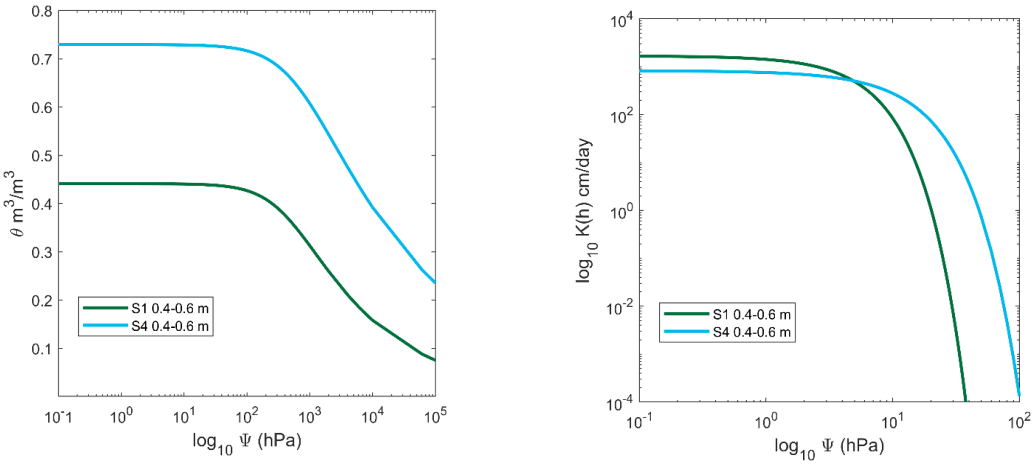

Fig. 33 SWRC and K(h) curves obtained at S1 and S2 (0.4-0.6 m).

To complete the characterization of the pilot site, the soil was analyzed for texture and chemical properties (Fig. 34). With this aim, disturbed soil samples were collected from each S location of Fig. 30 at the depth intervals 0–0.2 m, 0.2–0.4 m, 0.4–0.6 m, 0.6-0.8 m and analyzed

for texture, pH (1:2 soil-water extract), EC (1:5 soil–water extract), organic carbon (SOC), and exchangeable cations (Mg^{2+}, K^{+}, Na^{+}, and Ca^{2+}). Fig. 34 shows that the soil properties are highly variable among the stations. The sand % inside and outside the paleochannel increases in the south direction (S3 > S2 > S1 and S5 > S3), while the silt % follows the opposite trend. The clay % is almost constant. The average pH is around 7.5 in all stations with exception of S5 that is characterized by the greater peat content as demonstrated by the lower pH and the high SOC % and EC1:5. The amount of exchangeable cations corresponds to the variability in the EC1:5, with lower values of both parameters in the sandier S2 and S3, and the highest values found at S5.

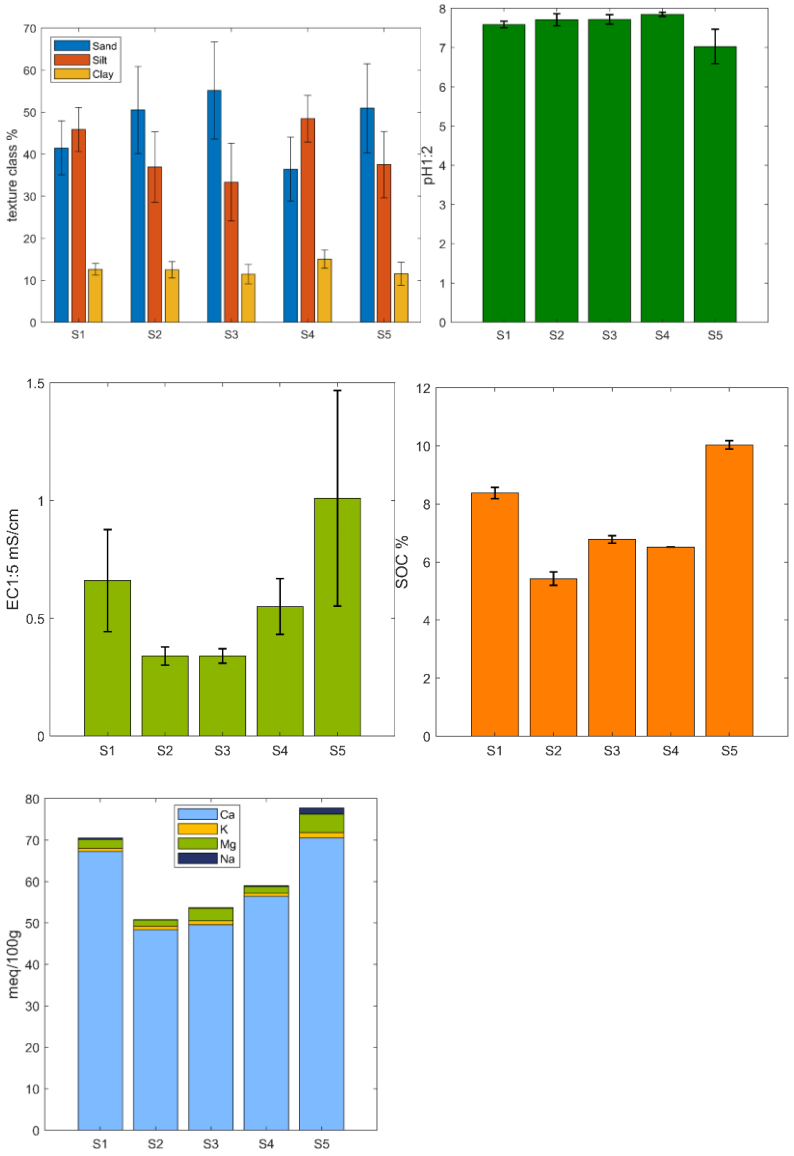

Fig. 34 Average texture, pH, EC, SOC, and exchangeable cations found at the five monitoring stations.

3.2 Chemical characterization of groundwater (M, T, P)

The chemical composition of groundwater is an important indicator of seawater intrusion and salinization processes. Seawater is mainly composed of Cl^-, Na^+, SO_4^{2-}, Mg^{2+}, Ca^{2+}, K^+, HCO_3^-, and Br^- with Cl^- and Na^+ accounting for 55% and 31 % of the total concentration. The study confirmed that the experimental site was strongly affected by soil and water salinity, and two major contamination dynamics were identified. Clear signals of seawater intrusion from the near lagoon and salty watercourses are the increase in water EC and Cl^-, and the Cl/Br ratio close to seawater value (= 648). In addition to seawater intrusion, the pilot site is affected by peat-driven salinization, particularly at the monitoring locations with high SOC and $SO_4^{2-} > Cl^-$. This second contribution was derived from the interactions between the peaty soil and salts that were originally in place since the area was reclaimed only a few decades ago (Zancanaro et al., 2020). The groundwater chemical monitoring consisted of weekly EC measurements and monthly analyses of major anions and cations. During the years 2019 and 2020, the sampling campaign was performed on S positions, while in 2021 the number of piezometers was increased including the P locations (Fig. 30). The observed variability of EC and ion concentrations in groundwater is shown in Fig. 35. Similar to what found in the soil analysis (see paragraph 5.1.1), the higher groundwater salinity (EC), Cl^-, and Na^+ were observed at S5 during 2019 and 2020. In 2021, the salinity of S1 and S3 increased with peaks that reached 20 mS/cm at S1, while S2 and S5 shows similar EC between the three years. The lowest amount of SO_4^{2-} was found at S1 that, on the other hand, is the location where the seawater intrusion phenomenon is more evident as demonstrated by the Cl/Br molar ratio identical to the seawater one. Lower ratios were observed at S2, S3, and S4 where the effects of saltwater intrusion are mitigated by freshening processes (e.g., rainfall events) that leach the salts. On the contrary, S5 has a Cl/Br ratio higher than 648, meaning that its salinity is driven by both seawater intrusion and leaching of the salts that are tied into the peaty soil.

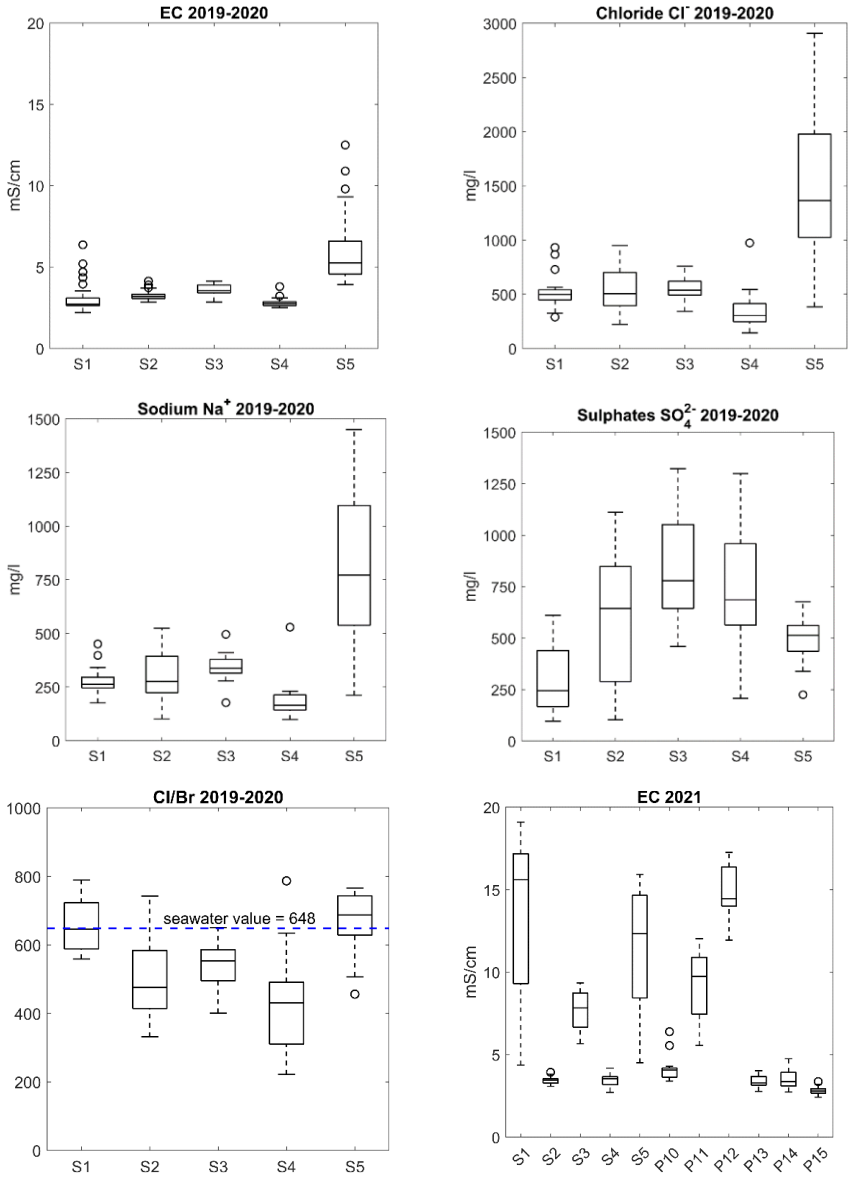

Fig. 35. Box plot showing the variability of EC, ions concentration, and depth to the water table. The line inside each box represents the median value; the upper and lower boundaries of each box represent the 25th and 75th quantiles; the dashed lines outside the boxes represent the expected data variability. Individual points are the outliers.

4. References

Albani A, Serandrei Barbero R, Donnici S (2007). Foraminifera as ecological indicators in the Lagoon of Venice, Italy. Ecological Indicators 7, 239-253, doi:10.1016/j.ecolind.2006.01.003

Boaga J, Viezzoli A, Cassiani G, Deidda G P, Tosi L, Silvestri S (2020). Resolving the thickness of peat deposits with contact-less electromagnetic methods: A case study in the Venice coastland. SCIENCE OF THE TOTAL ENVIRONMENT, 737, 139361, doi: 10.1016/j.scitotenv.2020.139361

Bonardi M, Tosi L, Rizzetto F, Brancolini G, Baradello L (2006). Effects of climate changes on the late Pleistocene and Holocene sediments of the Venice Lagoon, Italy. JOURNAL OF COASTAL RESEARCH, vol. SI 39, p. 279-284

de Franco R, Biella G, TOSI L., Teatini P, Lozej A, Chiozzotto B, Giada M, Rizzetto F, Claude C, Mayer A, Bassan V, Gasparetto-Stori G (2009). Monitoring the saltwater intrusion by time lapse electrical resistivity tomography: The Chioggia test site (Venice Lagoon, Italy). JOURNAL OF APPLIED GEOPHYSICS, 69; 117-130.

Donnici S, Serandrei-Barbero R, Bini C, Bonardi M, Lezziero A (2011). The Caranto Paleosol and its role in the early urbanization of Venice. Geoarchaeology: An International Journal 26(4):514-543

Lovrinović I, Bergamasco A, Srzić V, Cavallina C, Holjević D, Donnici S, Erceg J, Zaggia L, Tosi L (2021). Groundwater Monitoring Systems to Understand Sea Water Intrusion Dynamics in the Mediterranean: The Neretva Valley and the Southern Venice Coastal Aquifers Case Studies. Water, 13(4):561. https://doi.org/10.3390/w13040561

Rizzetto F, Tosi L, Carbognin L, Bonardi M, Teatini P (2003). Geomorphic setting and related hydrogeological implications of the coastal plain south of the Venice Lagoon, Italy. In Servat, E; Najem, W; Leduc, C; Shakeel, A, (Eds), HYDROLOGY OF MEDITERRANEAN AND SEMIARID REGIONS vol. 278, p. 463-470.

Rizzetto F, Tosi L, Zecchin M, Brancolini G, Baradello L, Tang C (2009). Ancient geomorphological features in shallows of the Venice Lagoon (Italy). JOURNAL OF COASTAL RESEARCH, vol. SI 56, p. 752-756

Rizzetto F, Tosi L, Zecchin M, Brancolini G (2010). Modern geological mapping and subsurface lithostratigraphic setting of the Venice Lagoon (Italy). RENDICONTI LINCEI. SCIENZE FISICHE E NATURALI, vol. 21, p. 239-252, doi: 10.1007/s12210-010-0085-1

Tosi L, Rizzetto F, Zecchin M, Brancolini G, Baradello L (2009). Morphostratigraphic framework of the Venice Lagoon (Italy) by very shallow water VHRS surveys: Evidence of radical changes triggered by human-induced river diversions. GEOPHYSICAL RESEARCH LETTERS, vol. 36, L09406, doi: 10.1029/2008GL037136

Tosi L, Rizzetto F, Bonardi M, Donnici S, Serandrei Barbero R, Toffoletto F. (2007). Note illustrative della Carta Geologica d'Italia alla scala 1: 50.000, Foglio 148-149 Chioggia-Malamocco, APAT, Dip. Difesa del Suolo, Servizio Geologico d'Italia, SystemCart, Roma, p. 164, 2 Maps

Tosi L, Teatini P, Brancolini G, Zecchin M, Carbognin L, Affatato A, Baradello L (2012). Three-dimensional analysis of the Plio-Pleistocene seismic sequences in the Venice Lagoon (Italy). JOURNAL OF THE GEOLOGICAL SOCIETY, vol. 169, p. 507-510, doi: 10.1144/0016-76492011-093

Zancanaro, E., Teatini, P., Sudiero, E., Morari, F., Identification of the origins of vadose zone salinity on an agricultural site in the Venice coastland by Ionic molar ratio analysis. Water, 12, 3363, doi:10.3390/w12123363, 2020.

Zecchin M, Caffau M, Tosi L (2011). Relationship between peat bed formation and climate changes during the last glacial in the Venice area. SEDIMENTARY GEOLOGY, vol. 238, p. 172-180, ISSN: 0037-0738, doi: 10.1016/j.sedgeo.2011.04.011

Zecchin M, Caffau M, Tosi L, Civile D, Brancolini G, Rizzetto F, Roda C (2010). The impact of Late Quaternary glacio-eustasy and tectonics on sequence development: evidence from both uplifting and subsiding settings in Italy. TERRA NOVA, vol. 22, p. 324-329, doi: 10.1111/j.1365-3121.2010.00953.x

Zecchin M, Brancolini G, Tosi L, Rizzetto F, Caffau M, Baradello L (2009). Anatomy of the Holocene succession of the southern Venice lagoon revealed by very high-resolution seismic data. CONTINENTAL SHELF RESEARCH, vol. 29, p. 1343-1359, doi: 10.1016/j.csr.2009.03.006